Structural Integrity Associates, Inc.® CALCULATION PACKAGE	File No.: 1400669.323
	Project No.: 1400669 Quality Program Type: ☒ Nuclear ☐ Commercial

PROJECT NAME:
Palisades Flaw Readiness Program for 1R24 NDE Inspection

CONTRACT NO.:
10426669

CLIENT:
Entergy Nuclear Operations, Inc.

PLANT:
Palisades Nuclear Plant

CALCULATION TITLE:
Crack Growth Analysis of the Cold Leg Bounding Nozzle

Document Revision	Affected Pages	Revision Description	Project Manager Approval Signature & Date	Preparer(s) & Checker(s) Signatures & Date
0	1 - 23 A-1 - A-2 Computer Files	Initial Issue	Norman Eng NE 5/11/15	Preparer: Wilson Wong WW 5/11/15 Checkers: Minji Fong MF 5/11/15 Gole Mukhim GSM 5/11/15

Table of Contents

List of Tables

List of Figures

1.0 OBJECTIVE

The objective of this calculation package is to determine maximum allowable flaw sizes for 18 and 36 months of continued operation based on crack growth analyses for a series of postulated flaws in the cold leg bounding nozzle boss weld in support of a Primary Water Stress Corrosion Cracking (PWSCC) susceptibility study at the Palisades Nuclear Plant (Palisades). The stresses due to the cold leg pipe interface loads which are determined in this calculation, and residual stresses extracted from a previous analysis [1], are used to calculate the stress intensity factors (K) which are used to perform crack growth analyses. The PWSCC crack growth analyses are performed using the **pc-CRACK** [2] program for both circumferential and axial flaws. The allowable detected flaw sizes are determined by back-calculating the predicted growth time to a maximum flaw size of 75% through wall thickness per ASME Code Section XI, IWB-3643.

2.0 DESIGN INPUTS

The finite element model shown in Figure 1 was developed in Reference [3] and is used for the determination of stress intensity factors.

2.1 Piping Interface Loads

Reference 4 [PDF file page 88] indicates that, for the cold leg, the bounding thermal transient stress is 7.307 ksi due to case Thermal 009, the deadweight (DW) stress is 0.459 ksi and the friction stress is 0.429 ksi. The cold leg loads are applied as an equivalent bending moment to the axial free end of the modeled cold leg. The equivalent bending moment is based on the combined stress which is assumed to occur at the outside surface of the cold leg. The maximum combined bending stress is:

DW + Friction + Thermal = 0.459 + 0.429 + 7.307 = 8.195 ksi

The moment based on the bending stress is calculated as:

$$M = \frac{\sigma \cdot I}{OR} = \frac{\pi}{4} \cdot \frac{(17.84375^4 - 14.84375^4) \cdot 8.195}{17.84375} = 19056 \ \textit{in-kips}$$

where,

M = moment applied to the free end of the cold leg
σ = stress on the cold leg pipe
I = Moment of Inertia – $(\pi/4)(OR^4 - IR^4)$
IR = Inside radius of nozzle (in) = 14.84375" [3]
OR = Outside radius of nozzle (in) = 17.84375 [3]

Since half the cold leg pipe is modeled, the equivalent moment applied to the model is 9528 in-kips (= 19056 in-kips /2). The moment is applied to the axial free end of the cold leg run piping by means of a pilot node pair to transfer the loading. The pilot node pair is composed of a target node at the center of the pipe (ANSYS TARGE170 element) and a set of surface contact elements on the axial end of the pipe (ANSYS CONTA174 element). The surface elements are bonded to the pilot node in a slave/master coupling relationship, so that the moment load applied to the pilot node is transferred to the end of the pipe. The cold leg bounding nozzle piping loads are considered to have negligible effects on the resulting K's for the boss weld, and are therefore not considered.

2.2 Residual Stresses at Normal Operating Temperature and Pressure

Residual stresses at the fifth operating condition cycle (at time = 2106 minutes) are taken from Reference [1]. These stresses include the effects of normal operating temperature of 537°F and pressure of 2085 psig [1].

2.3 Mechanical Load Boundary Conditions

The mechanical load boundary conditions for the stress analyses are symmetric boundary conditions at the symmetry planes of the model, axial displacement restraint at the end of the nozzle, and axial displacement restraint on the pilot node, as shown in Figure 2. In the case where axial flaws are modeled on the symmetry planes, the boundary conditions are released at the nodes where the flaw exists.

2.4 Crack Growth Rate

The default PWSCC growth rate in **pc-CRACK** [2] is used. This relation is based on expressions in Reference [5, Section 4.3] and the resulting equation for the crack growth rate is as follows:

$$\frac{da}{dt} = C \exp\left[-Q\left(\frac{1}{T+460} - \frac{1}{T_{ref}+460}\right)\right](K - K_{th})^{\beta} \qquad \text{for} \quad K > K_{th}$$

For times (t) in hours, temperatures (T and T_{ref}) in °F, crack length (a) in inches and K in ksi-√in, the following reference values are used:

T_{ref} = 617°F

$C = 2.47\text{x}10^{-7}$ (constant)

β = 1.6 (constant)

Q = 28181.8°R (constant)

K_{th} = 0 (threshold stress intensity factor below which there is no crack growth)

T = operating temperature at location of crack

3.0 ASSUMPTIONS

The following assumptions are used in this analyses:

- The cold leg bounding nozzle piping loads are not considered in calculating stress intensity factors since loads on the nozzle do not produce Mode I crack opening stress intensity factors that contribute to crack growth in the boss weld.
- The maximum combined stress on the cold leg piping is assumed to occur at the outside surface of the cold leg.

4.0 DETERMINATION OF STRESS INTENSITY FACTOR

The stresses described in this section are used with a modified version of the finite element model (FEM) developed previously in Reference [3] to determine stress intensity factors. The modification of the FEM consists of adding crack tip elements as addressed in Section 4.2 and 4.3. The stress intensity factors (Ks) are calculated using the KCALC feature in ANSYS [6] which is based on the linear elastic fracture mechanics (LEFM) principles. For the LEFM evaluations, only the elastic properties are used in the FEA.

4.1 Crack Face Pressure Application

In order to determine the Ks for the circumferential and axial flaws due to residual stresses, the stresses on the boss weld-to-nozzle interface, at the fifth operating condition (at time = 2106 minutes in the residual stress analysis [1]), are extracted from the residual stress analysis and reapplied on the crack face as surface pressure loading.

This approach is based on the load superposition principle [7], which is utilized to transfer the stresses from the weld residual stress finite element model onto the fracture mechanics finite element model that contains crack tip elements. The superposition technique is based on the principle that, in the linear elastic regime, stress intensity factors of the same mode, which are due to different loads, are additive (similar to stress components in the same direction).

The superposition method can be summarized with the following sketches [7, page 66]:

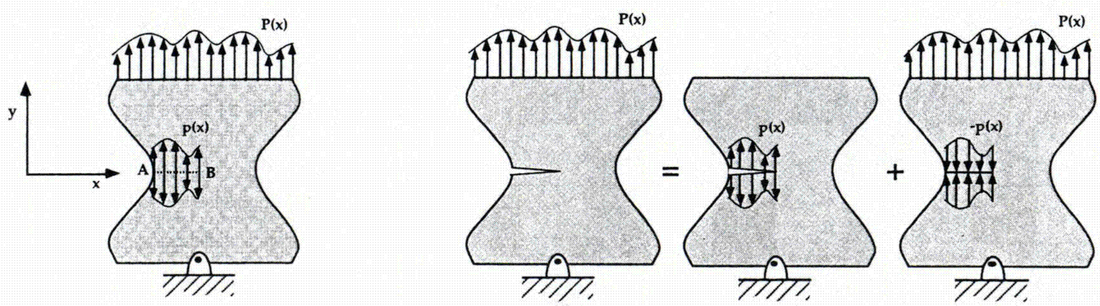

(a) (b) (c) (d)

A load p(x) on an uncracked body, Sketch (a), produces a normal stress distribution p(x) on Plane A-B. The superposition principle is illustrated by Sketches (b), (c), and (d) of the same body with a crack at Plane A-B. The stress intensity factors resulting from these loading cases are such that:

$K_I(b) = K_I(c) + K_I(d)$

Thus, $K_I(d) = 0$ because the crack is closed, and:

$K_I(b) = K_I(c)$

This means that the stress intensity factor obtained from subjecting the cracked body to a nominal load p(x) is equal to the stress intensity factor resulting from loading the crack faces with the same stress distribution p(x) at the same crack location in the uncracked body.

4.2 K Calculation for Circumferential Flaws

4.2.1 Finite Element Model with Circumferential Flaws

The stress intensity factors for full circumferential flaws in the nozzle boss weld are determined by finite element analysis using deterministic linear elastic fracture mechanics (LEFM) principles. As a result, five fracture mechanics finite element models are derived to include "collapsed" crack meshing that represent full (360°) circumferential flaws surrounding the nozzle at various depths within the boss weld.

The circumferential flaws align with the interface between the boss weld and the nozzle. The modeled flaw depths are: 0.13", 0.88", 1.45", 2.32", and 2.99" as measured at the 0° axial side of the cold leg pipe.

The modeling of the flaws, or cracks, involves splitting the crack plane and then inserting "collapsed" mesh around the crack tips followed by concentrated mesh refinements that surround the "collapsed" mesh, and are referred to as "crack tip elements". This step is implemented on a source finite element model without the cracks (the FEM developed in Reference 3) where crack tip elements are inserted by an in-house developed ANSYS macro.

For the fracture mechanics models, 20-node quadratic solid elements (ANSYS SOLID95) are used in the crack tip region, while 8-node solid elements (ANSYS SOLID185) are used everywhere else in the model. The mid-side nodes for the SOLID95 elements around the crack tips are shifted to the "quarter point" locations to properly capture the singularities at the crack tips, consistent with ANSYS recommendations. The finite element model for the 2.99" deep circumferential flaw, with the crack tip mesh, is shown in Figure 3 as an example; the crack tip mesh for the other crack depths follows the same pattern.

The quarter point mid-side nodes combined with the extra layers of concentrated elements around the crack tips provide sufficient mesh refinement to determine the stress intensity factors for the fracture mechanics analyses.

4.2.2 Stress Intensity Factor Results

The radial stresses (radial to the nozzle axis) on the weld/nozzle interface are transferred to the circumferential flaws as crack face pressure per the superposition principle described in Section 4.1.

Figure 4 depicts, as an example, the transferred radial stresses as crack face pressure for the 2.99" circumferential crack depth. During the crack face pressure transfer, the operating pressure of 2085 psi is added to the crack face pressure to account for the internal pressure acting on the crack face due to cracking. A far field in-plane bending moment per Section 2.1 is also applied to the free end of the cold leg run piping to account for the pipe moment in the main loop piping.

Each crack model is analyzed as a steady state stress pass at the operating and reference temperature of 537°F [1] in order to use the material properties at the operating temperature, but without inducing additional thermal stresses.

At the completion of each analysis, the ANSYS KCALC post-processing is performed to extract the K's at each crack tip node around the nozzle. The maximum K results are summarized in Table 1 for various crack depth ratios "a/t". Since the crack tip location is same in the circumferential flaw, the maximum K from all locations at each crack size is conservatively used for the K vs. a profile. The "K vs. a/t" trends are then plotted in Figure 5.

4.3 K Calculation for Axial Flaws

4.3.1 Finite Element Model with Axial Flaws

The stress intensity factors for axial flaws are determined using the same methodology as the circumferential flaws. However, the mesh of weld nuggets was removed to insert thumbnail shape flaws in the model. Also, the orientation and shape of the flaws allow all crack depths at the 0° and 90° faces of the symmetric cold leg pipe model to be inserted simultaneously. Figure 6 shows the five modeled crack depths (0.25", 0.78", 1.37", 2.16", and 2.90") on the 0° face (cold leg axial face) and 90° face with crack tip elements inserted.

The modeling of the axial flaws uses the same crack tip elements as described in Section 4.2.1. The crack tip mesh is the same pattern used in the circumferential flaws and is shown in Figure 6 for the axial flaws at the 0° and 90° faces.

4.3.2 Stress Intensity Factor Results

Similar to the circumferential flaw analyses, the crack opening residual stresses and additional operating pressure are transferred to the axial flaws as crack face pressure. Figure 7 depicts, as an example, the

transferred hoop stresses as crack face pressure for the axial flaws. In addition, a far field in-plane bending moment per Section 2.1 is also applied to the free end of the cold leg run piping to account for the pipe moment in the main loop piping. The K results at the deepest point of the flaws are summarized in Table 2 for various crack depth ratios "a/t" and plotted in Figure 8. Since the deepest point of the postulated axial flaws has the smallest remaining wall thickness, the K at the deepest point is used for the K vs a profile.

5.0 CRACK GROWTH CALCULATION

Stress intensity factors (Ks) at four depths for 360° inside surface connected, part-through-wall circumferential flaws as well as two axial thumbnail flaws at the 0-and 90-degree azimuthal locations of the nozzle, are calculated using finite element analysis (FEA). For the circumferential flaw, the maximum K values around the nozzle circumference for each flaw depth are extracted and used as input into **pc-CRACK** to perform the PWSCC crack growth analyses. For the axial flaws, the K at the deep point of the thumbnail shape is used as input for performing the PWSCC crack growth analyses. Since the K vs. a profile is used as input, the shape of the component is not relevant.

For the crack growth analyses, two initial flaw sizes were chosen. These are based on expected engineering flaw sizes that could be present for a crack that would then grow by PWSCC. The final flaw size for these analyses is 75% of the wall thickness. This final depth is chosen as it is the maximum allowable flaw depth per Section XI of the ASME Code for pipe flaw evaluations. Additionally, a final flaw size of 95% of the wall thickness is also considered in this calculation.

The following are the additional parameters needed for the crack growth calculations:

Two initial crack depths = 0.025" and 0.1" (assumed)
Temperature = 537°F (operating temperature [1])
Wall thickness = 3" (Cold Leg thickness [3])

The resulting crack depths for the circumferential and axial flaws, as a function of time, as calculated by **pc-CRACK** are shown in Figure 9 for the 0.025" initial flaw size and Figure 10 for the 0.1" initial flaw size. The time for a flaw to grow from the initial flaw size to 75% and 95% though-wall is tabulated in Table 3 and Table 4 for both circumferential and axial flaw types, respectively. Table 5 shows the allowable detected flaw sizes for the postulated flaws if continued operation for 18 and 36 months is considered.

6.0 CONCLUSIONS

Stress intensity factors were calculated for the 360° circumferential flaws as well as the axial flaws at the 0° and 90° locations. The stress intensity factors were calculated using residual stress distributions for residual stress plus normal operating conditions. In addition, a far field in-plane bending moment is

applied to the free end of the cold leg run piping to account for piping moments in the main loop piping. This combined loading is used for the determination of the stress intensity factors for both the circumferential and axial flaws. Figure 5 and Figure 8 as well as Table 1 and Table 2, show the calculated stress intensity factors for the circumferential and axial flaws.

Crack growth evaluations were performed for circumferential and axial flaw configurations using two different initial flaw sizes. As shown in Figure 9 and Table 3, the shortest time for an initial 0.025" deep flaw to grow to 75% through-wall in all cases is 55.6 years for a circumferential flaw. Figure 10 and Table 3 show that the shortest time for an initial 0.1" deep flaw to grow to 75% through-wall in all cases is 53.5 years for a circumferential flaw. Table 5 shows the maximum allowable detected flaw sizes for 18 and 36 months of continued operation.

7.0 REFERENCES

1. SI Calculation No. 1400669.322, Rev. 0, "Cold Leg Bounding Nozzle Weld Residual Stress Analysis."
2. **pc-CRACK 4.1**, Version 4.1 CS, Structural Integrity Associates, December 2013.
3. SI Calculation No. 1400669.320, Rev. 0, "Finite Element Model Development for the Cold Leg Drain, Spray, and Charging Nozzles."
4. Palisades Document, Report No. CENC-1115, "Analytical Report for Consumers Power Piping," SI File No. 1300086.204.
5. *Materials Reliability Program: Crack Growth Rates for Evaluating Primary Water Stress Corrosion cracking (PWSCC) of Alloy 82, 182 and 132 Welds (MRP-115),* EPRI, Palo Alto, CA: 2004, 1006696.
6. ANSYS Mechanical APDL and PrepPost, Release 14.5 (w/ Service Pack 1), ANSYS, Inc., September 2012.
7. Anderson, T. L., "Fracture Mechanics Fundamentals and Applications," Second Edition, CRC Press, 1995.

Table 1: Stress Intensity Factors for Circumferential Flaws

Depth (in)	a/t	Max K (ksi-in^0.5)
0.13	0.04	22.07
0.83	0.28	28.50
1.42	0.47	20.84
2.31	0.77	20.97
2.99	1.00	48.27

Table 2: Stress Intensity Factors for Axial Flaws

CL Axial Plane 0°			CL Circ. Plane 90°		
Crack Depth (in)	a/t	K at Deep Pt (ksi-in$^{0.5}$)	Crack Depth (in)	a/t	K at Deep Pt (ksi-in$^{0.5}$)
0.25	0.08	21.26	0.24	0.08	18.43
0.78	0.26	20.95	0.83	0.28	19.00
1.37	0.46	19.58	1.43	0.48	20.82
2.16	0.72	22.89	2.19	0.73	25.67
2.90	0.97	28.34	2.85	0.95	30.93

Table 3: Crack Growth Time to 75% Through-Wall

Initial Flaw Size (in)	Axial Crack (0° plane) (years)	Axial Crack (90° plane) (years)	Circ. Crack (years)
0.025	64.5	67.2	55.6
0.100	62.2	64.4	53.5

Table 4: Crack Growth Time to 95% Through-Wall

Initial Flaw Size (in)	Axial Crack (0° plane) (years)	Axial Crack (90° plane) (years)	Circ. Crack (years)
0.025	77.0	77.9	66.2
0.100	74.6	75.0	64.0

Table 5: Allowable Detected Flaw Size

Allowable Detected Flaw Size (a/t) Cold Leg Thickness, t = 3.00"						
Months of Continued Operation	**Axial Flaw at 0° plane**		**Axial Flaw at 90° plane**		**Circumferential Flaw**	
	a/t	**a (in)**	**a/t**	**a (in)**	**a/t**	**a (in)**
18	0.7238	2.1715	0.7202	2.1605	0.7269	2.1807
36	0.6871	2.0613	0.6788	2.0363	0.6273	1.8818

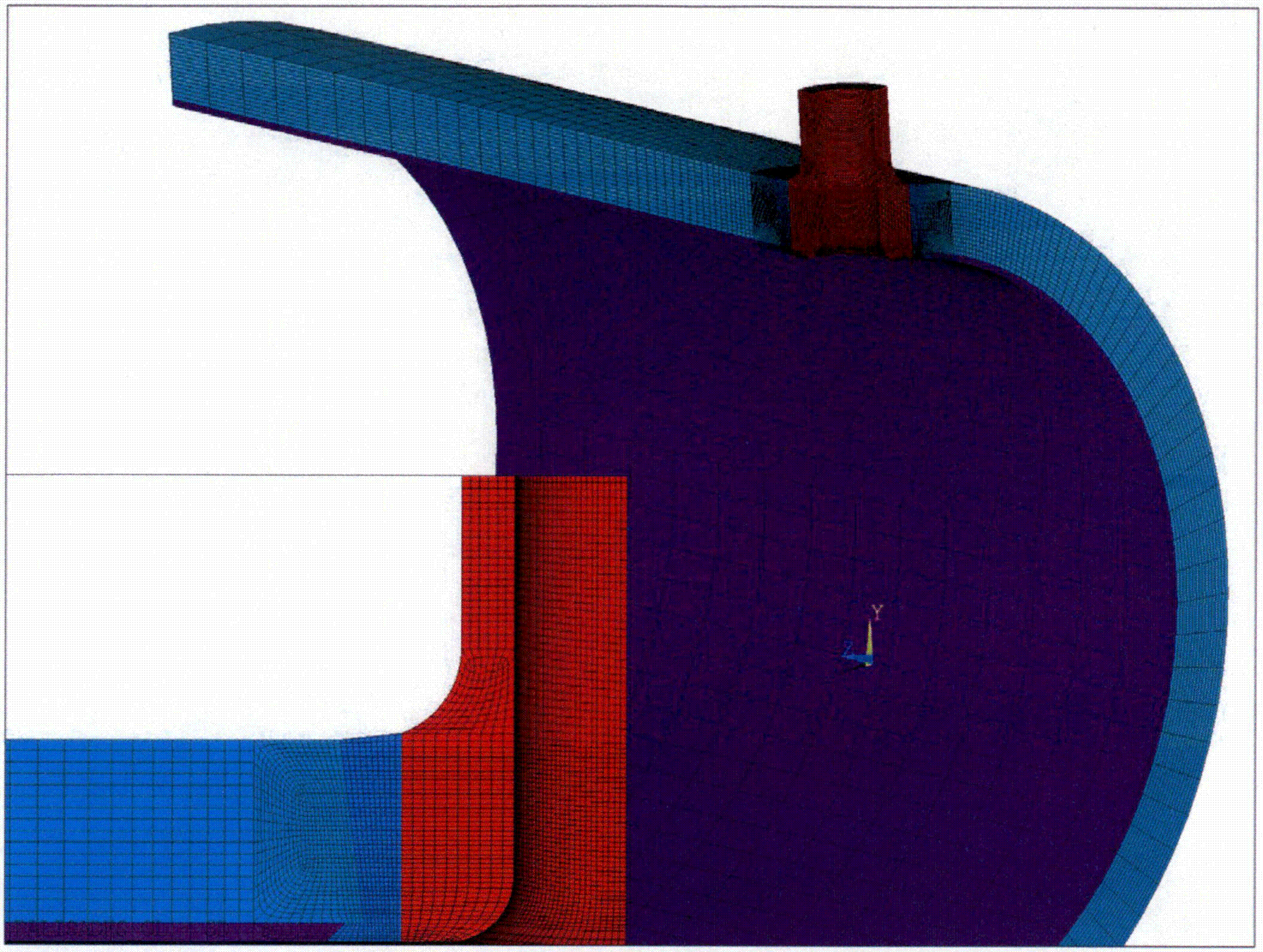

Figure 1. Base Finite Element Model Mesh

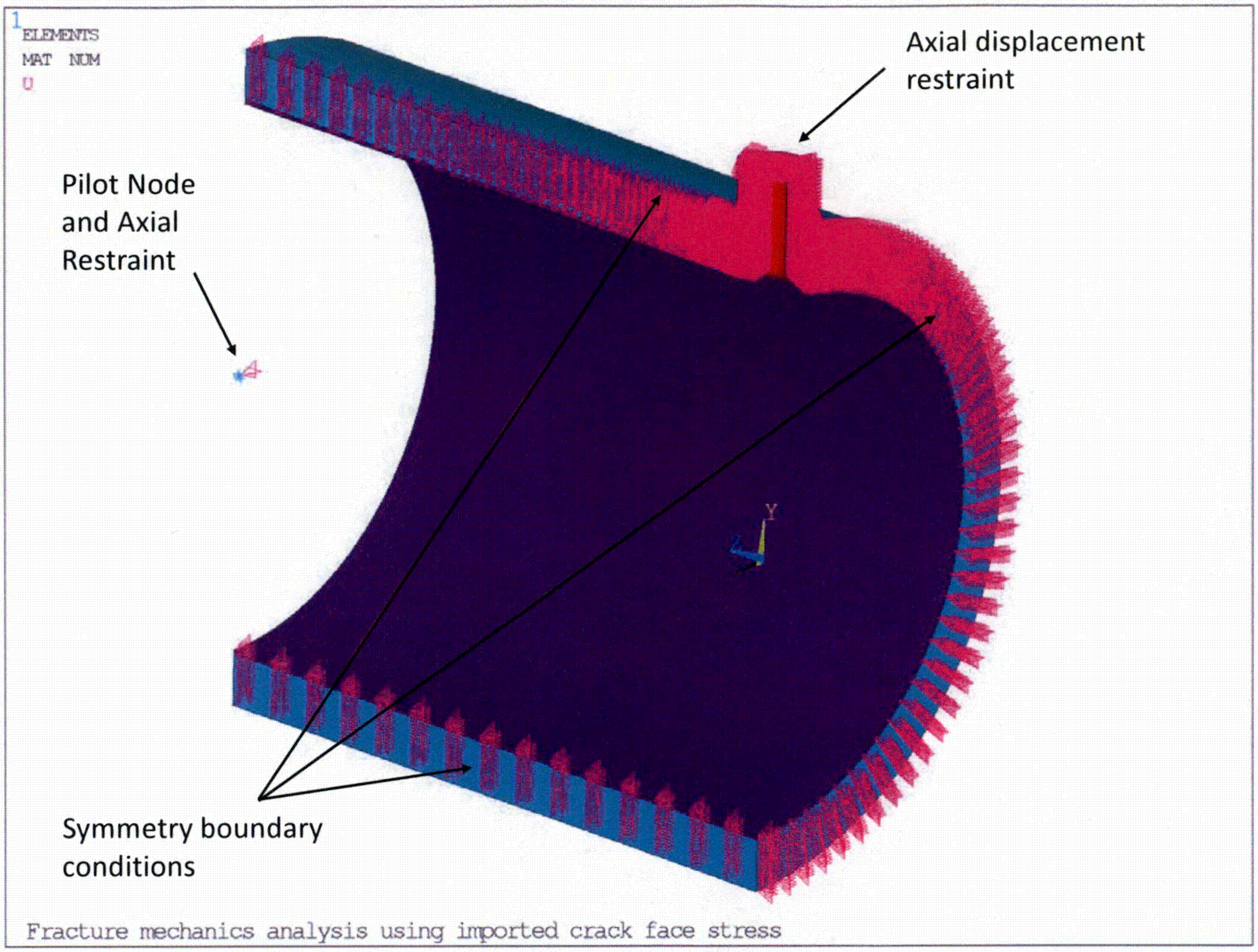

Figure 2. Applied Mechanical Load Boundary Conditions

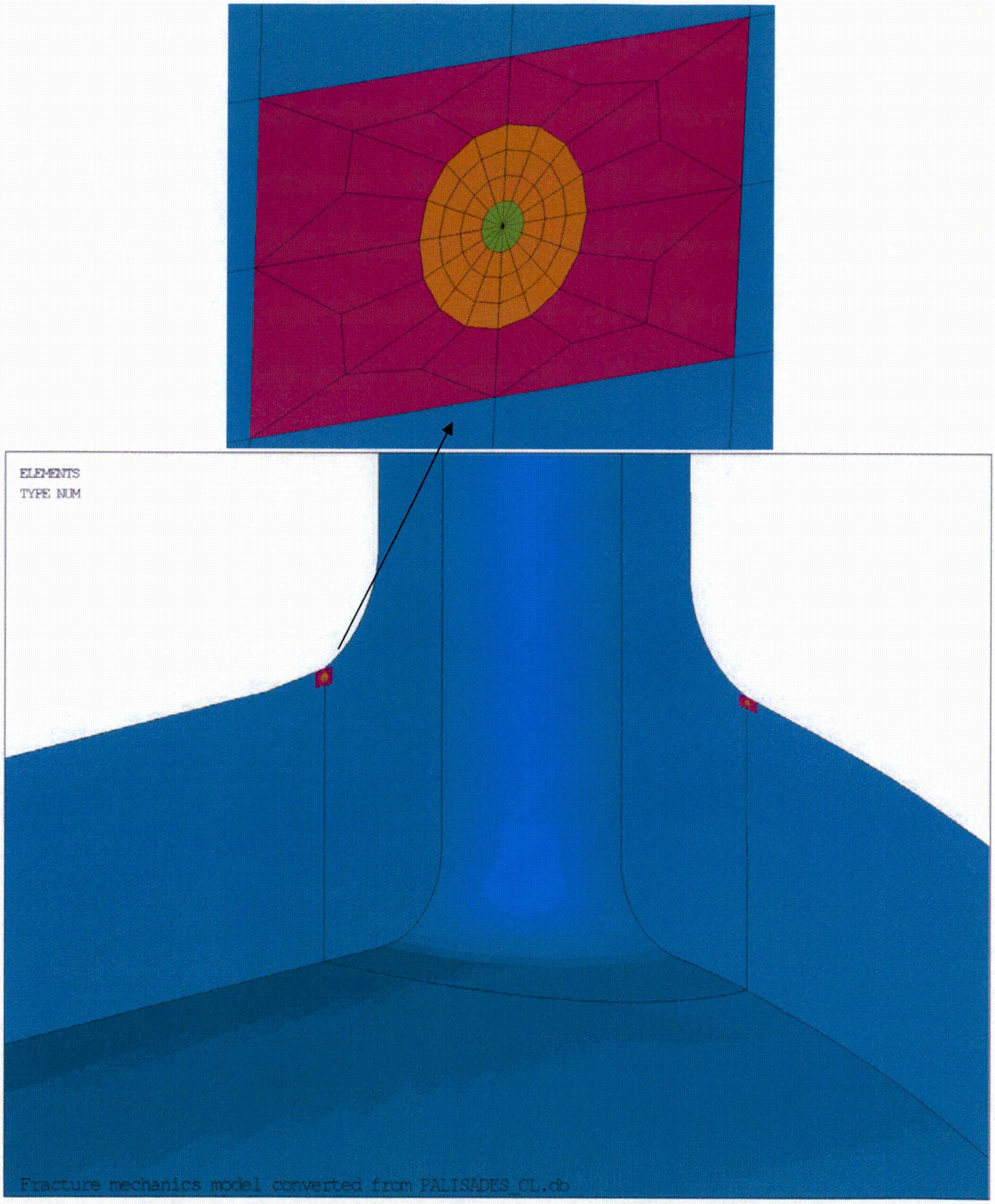

Figure 3. Circumferential Flaw with Crack Tip Elements Inserted

(Note: Deepest circumferential flaw shown for example)

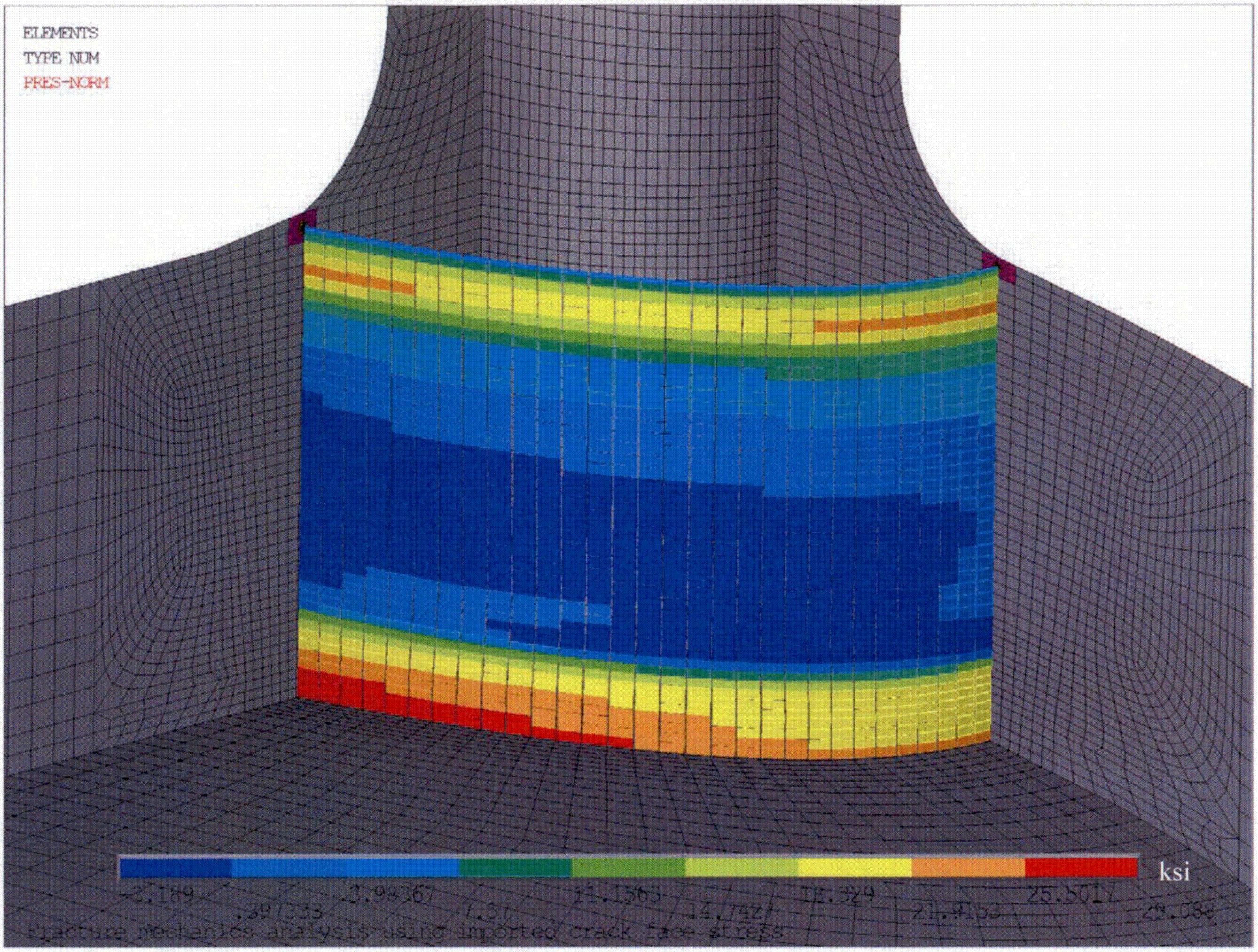

Figure 4. Transferred Residual Stress + NOC + Pressure Stress for Circumferential Flaws

(Note: Deepest circumferential flaw shown for example)

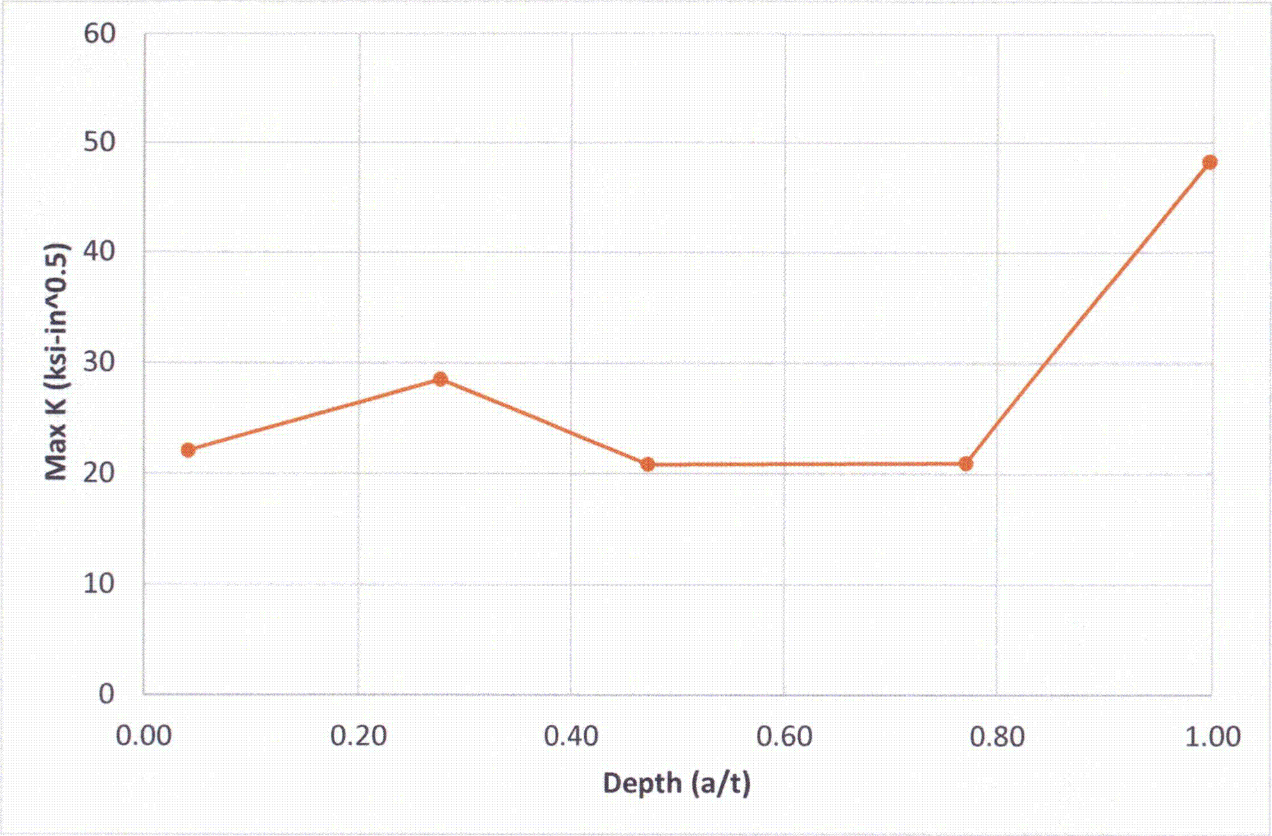

Figure 5. Stress Intensity Factors as a Function of Depth for Circumferential Flaws

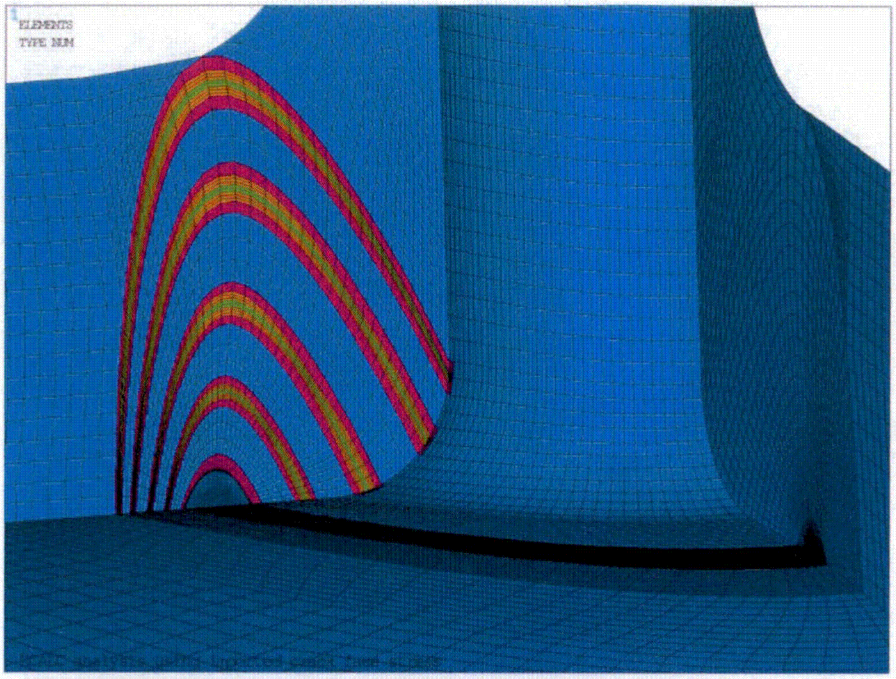

0° plane

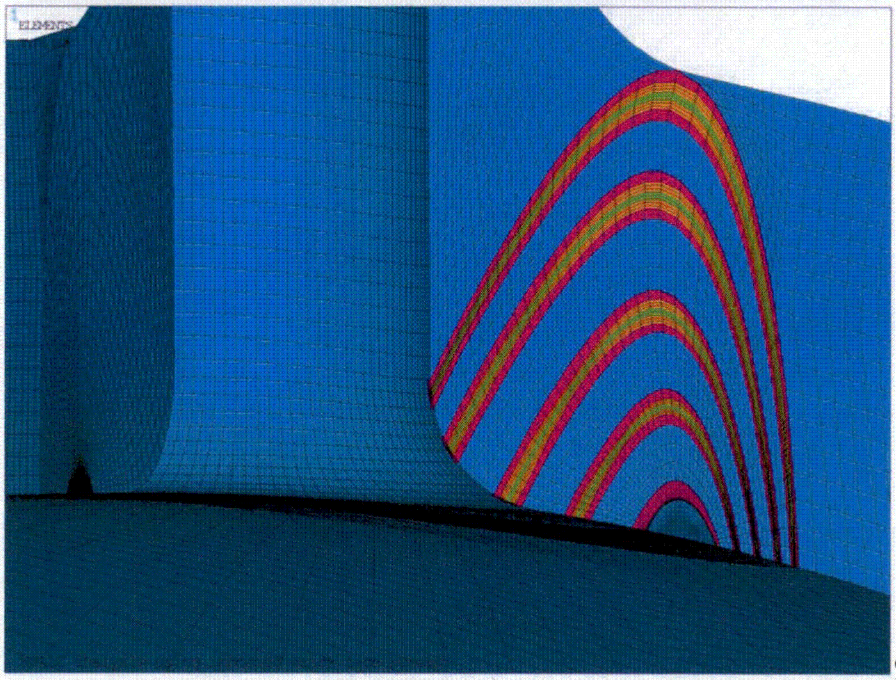

90° plane

Figure 6. Axial Flaws with Crack Tip Elements Inserted

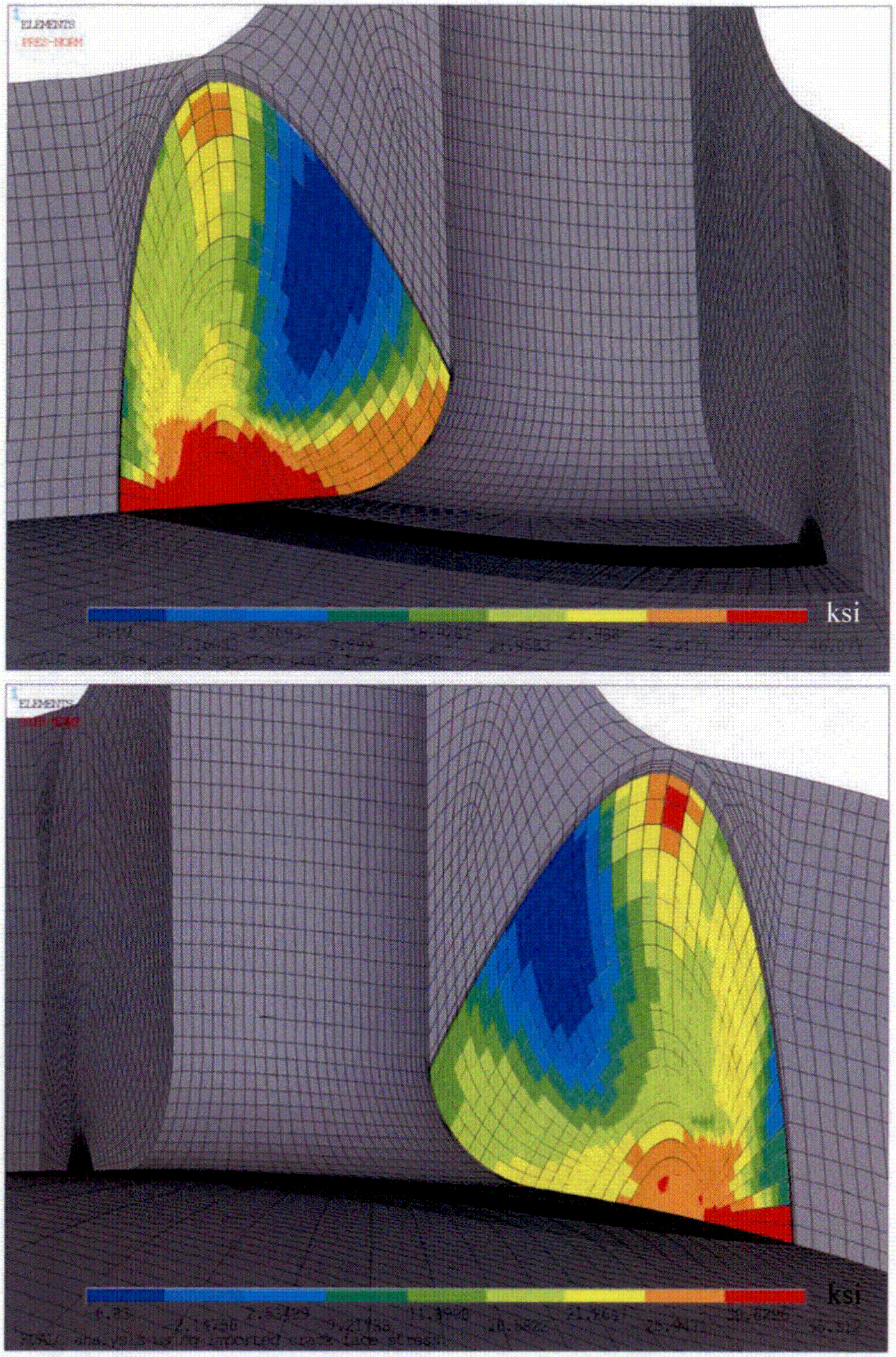

0° plane

90° plane

Figure 7. Transferred Residual Stress + NOC + Pressure Stress for Axial Flaws

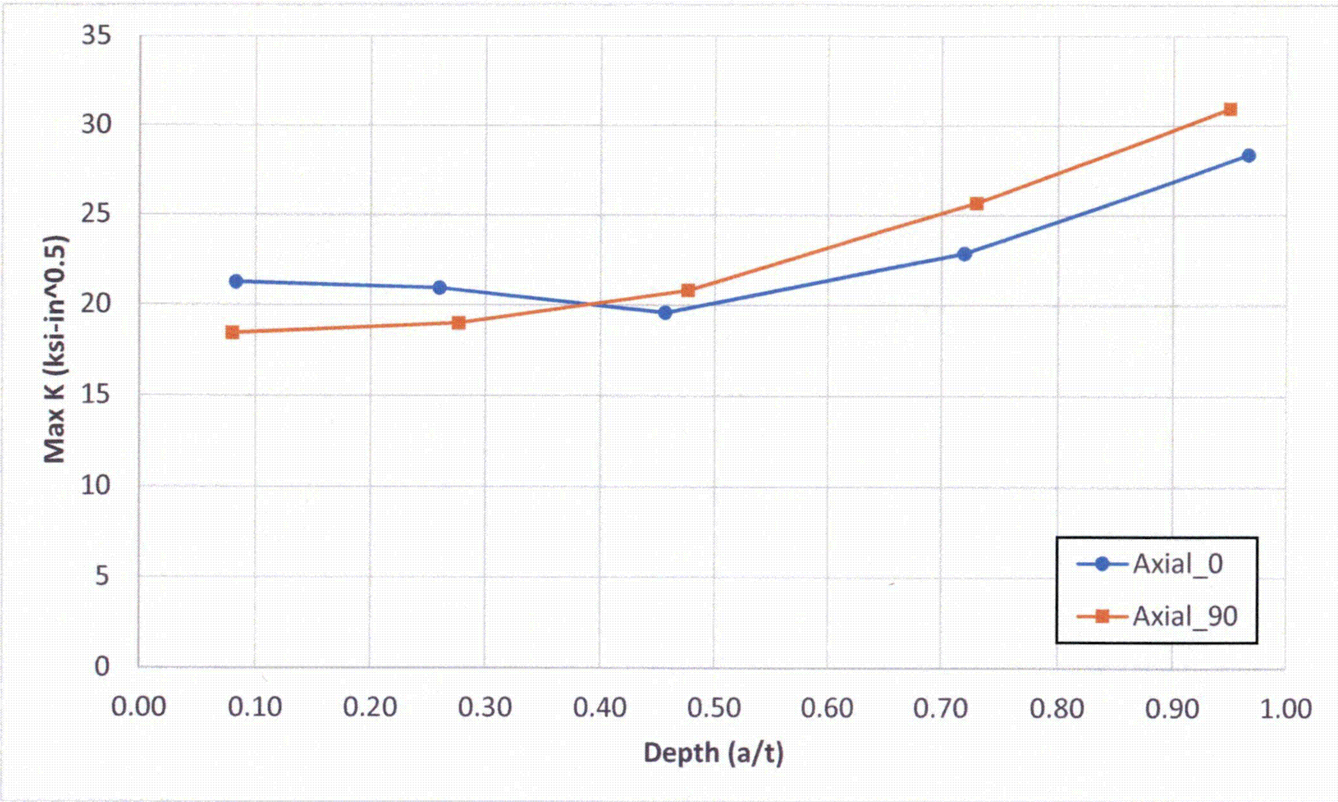

Figure 8. Stress Intensity Factors as a Function of Depth for Axial Flaws

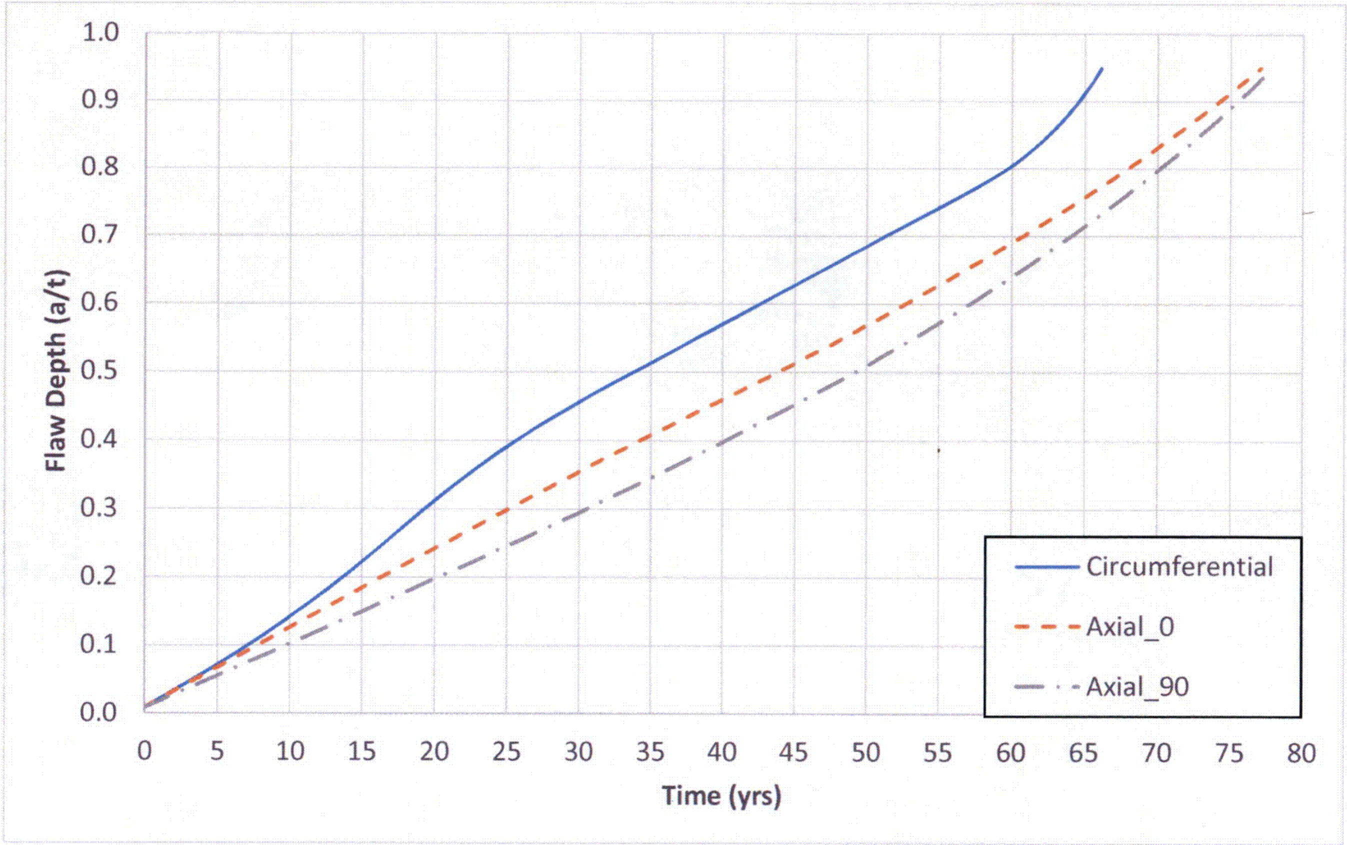

Figure 9. Crack Growth for All Flaw Types with 0.025" Initial Flaw Size

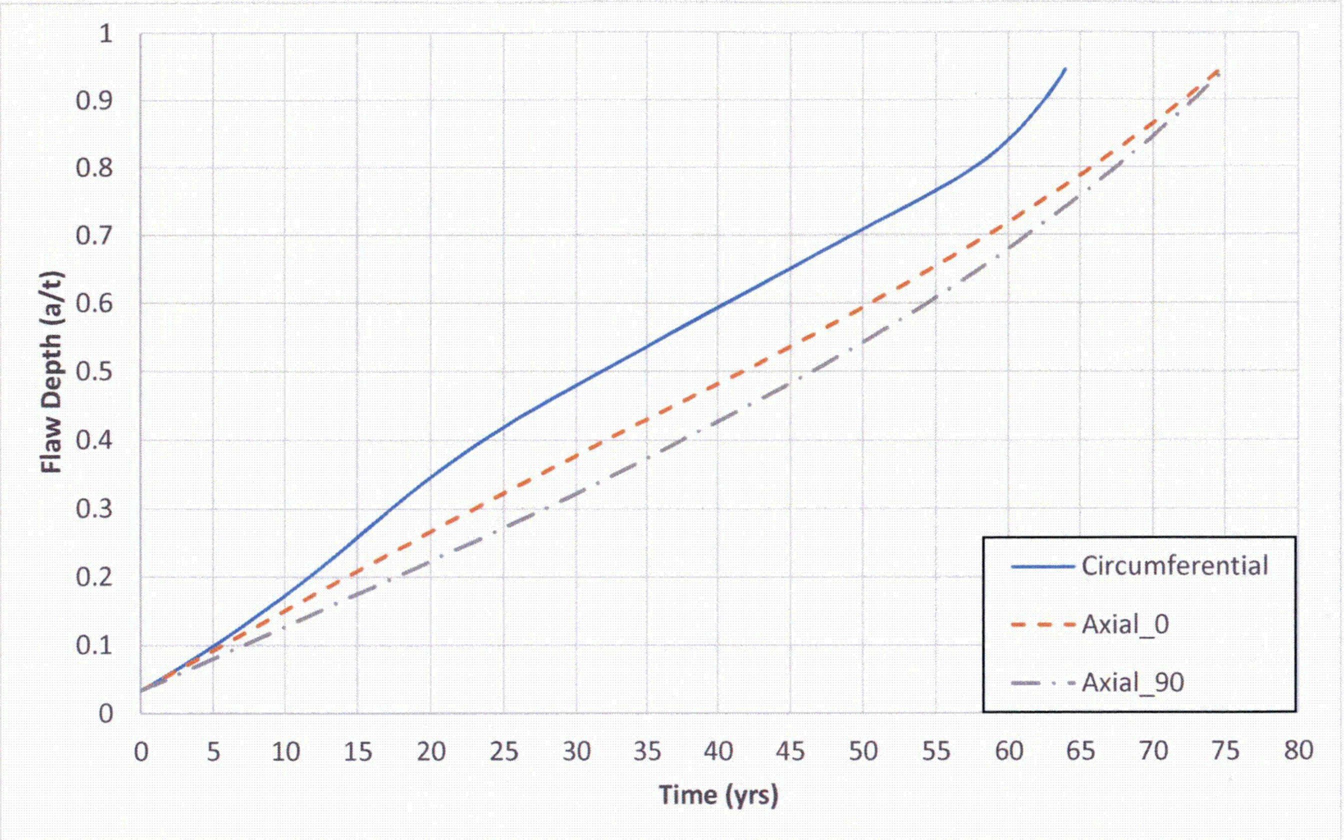

Figure 10. Crack Growth for All Flaw Types with 0.1" Initial Flaw Size

APPENDIX A

COMPUTER FILE LISTING

File	Description
Palisades_CL.DB	Base model geometry for crack tip insertion [3]
CL_axial.INP	Input file to modify base mesh for axial crack tip insertion
BCNODES.INP	Input file for nodal component definitions
FM_CL_AXL*.INP	Geometry input files to create circumferential flaw at specified depth. * = 05, 30, 50, 75, and 95
FM_CL_AXL*_COORD.INP	Input files to determine circumferential crack face element centroid coordinates. * = 05, 30, 50, 75, and 95
FM_CL_AXL*_GETSTR.INP	Input files to extract circumferential crack face stresses from residual stress analysis. * = 05, 30, 50, 75, and 95
FM_CL_AXL*_IMPORT.INP	Input files to transfer stresses into circumferential crack face pressure (plus operating pressure on crack face and applied pipe moment). * = 05, 30, 50, 75, and 95
Axial*_Nodes.INP	Crack tip definition file for axial cracks
FM_PALISADES_CL_C#.INP	Geometry input files to create circumferential flaw at specified depth. # = 05, 30, 50, 75, and 95
FM_PALISADES_CL_C#_COORD.INP	Input files to determine circumferential crack face element centroid coordinates. # = 05, 30, 50, 75, and 95
FM_PALISADES_CL_C#_GETSTR.INP	Input files to extract circumferential crack face stresses from residual stress analysis. # = 05, 30, 50, 75, and 95
FM_PALISADES_CL_C#_IMPORT.INP	Input files to transfer stresses into circumferential crack face pressure (plus operating pressure on crack face and applied pipe moment). # = 05, 30, 50, 75, and 95
NodesC#.INP	Crack tip definition file for circumferential cracks
STR_FieldOper_STR_C##1.txt	Extracted circumferential crack face stresses from residual stress analysis. ## = 05, 30, 50, 75, and 95
STR_FieldOper_Axl**1.txt	Extracted axial crack face stresses from residual stress analysis. ** = 00, and 90
FM_CL_AXL**_IMPORT_K.CSV	Formatted K result outputs for axial crack. ** = 00, and 90
FM_PALISADES_CL_C##_IMPORT_K.CSV	Formatted K result outputs for circumferential crack. ## = 05, 30, 50, 75, and 95
CircFlaw_$$$$.pcf	**pc-CRACK** PWSCC growth input file for circ flaw. $$$$ = 0025 and 01, 0025 = 0.025" and 01 = 0.1" initial flaw size
AxialFlaw_0_$$$$.pcf	**pc-CRACK** PWSCC growth input file for axial flaw on 0° plane. $$$$ = 0025 and 01
AxialFlaw_90_$$$$.pcf	**pc-CRACK** PWSCC growth input file for axial flaw on 90° plane. $$$$ = 0025 and 01
CircFlaw_$$$$.rpt	**pc-CRACK** PWSCC growth output file for circ flaw. $$$$ = 0025 and 01
AxialFlaw_0_$$$$.rpt	**pc-CRACK** PWSCC growth output file for axial flaw on 0° plane. $$$$ = 0025 and 01
AxialFlaw_90_$$$$.rpt	**pc-CRACK** PWSCC growth output file for axial flaw on 90° plane. $$$$ = 0025 and 01